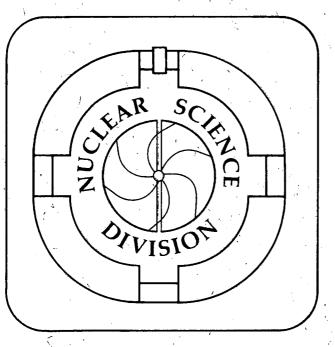# Lawrence Berkeley Laboratory

UNIVERSITY OF CALIFORNIA

To be submitted for publication

Scaling Laws, Shell Effects and Transient Times in Fission Probabilities

L.G. Moretto, K.X. Jing, R. Gatti, G.J. Wozniak, and R.P. Schmitt

July 1995

DISCLAIMER

Scaling Laws, Shell Effects and Transient Times in Fission Probabilities

L.G. Moretto, K.X. Jing, R. Gatti, and G.J. Wozniak

Nuclear Science Division, Lawrence Berkeley Laboratory
University of California, Berkeley, CA 94720, USA

R.P. Schmitt

Cyclotron Institute, Texas A&M University, College Station, TX 77843-3366

July 1995

Scaling Laws, Shell Effects and Transient Times in Fission Probabilities

L. G. Moretto, K. X. Jing, R. Gatti[a], and G. J. Wozniak

Nuclear Science Division, Lawrence Berkeley Laboratory,
University of California, Berkeley, California 94720

R. P. Schmitt

Cyclotron Institute, Texas A&M University, College Station, TX 77843-3366

Abstract: The fission excitation functions for fourteen compound nuclei covering a mass range from A = 186 - 213 are shown to scale exactly according to the transition state prediction once shell effects are accounted for. The extracted shell effects correlate closely with those obtained from the ground state masses. No effects of transient times longer than 3×10^{-20} seconds are visible. Pairing effects are noticeable at excitation energies a few MeV above the barrier.

Fission excitation functions vary dramatically from nucleus to nucleus as one scans across the nuclide chart. Some of these differences are readily understood in terms of a changing liquid-drop fission barrier. Others are obviously associated with the strong shell effects in the neighborhood of the doubly magic numbers 82 protons and 126 neutrons, and with their disappearance with excitation energy. Additional effects may be associated with pairing, angular momentum dependence of the fission barriers, etc.

The standard attempts to interpret these excitation functions have been based upon the transition state rate for fission[1]. The recent literature, however, provides extensive claims for the failure of the transition state rates to account for the measured amounts of pre-scission neutrons or γ-rays in relatively heavy fissioning systems[2-4] . This alleged failure has been attributed to the transient time necessary for the "slow" fission mode to attain its

stationary decay rate[5-12]. A suitably short total compound nucleus lifetime would manifest this transient time through a substantially reduced fission probability.

In this paper we are going to show the following: a) fission excitation functions for nuclei ranging from A=186 to 213 are rigorously scalable in terms of the transition state rates; b) this scaling requires the knowledge of an effective fission barrier B_f^* and a shell correction Δ_{shell}; c) the shell corrections Δ_{shell} obtained from the data are in excellent agreement with those obtained from the ground state masses; d) no transient times longer than $\sim 3 \times 10^{-20}$ sec are apparent from the scaled excitation functions.

A recent paper[13] has analyzed intermediate mass fragment excitation functions for an extensive range of fragment atomic numbers, obtained for four different compound nuclei. A special way of plotting these data permits the ready observation of deviations from the transition state rates as a departure from a 45° straight line. For over 70 excitation functions, the lack of deviations from the transition state null hypothesis both as a function of fragment Z and excitation energy led to the conclusion that the transition state rates were closely obeyed, and that no substantial transient time effects were present in these systems over the covered experimental energy and lifetime ranges.

It would be interesting to extend this method to the fission of systems closer in mass to those for which transient time effects have been claimed[2, 3]. A large number of fission excitation functions is available in the literature[14-17] over an extended energy range in the mass region $186 \leq A \leq 213$. An equally large number of yet unpublished excitation functions has recently surfaced from our files. These excitation functions are of special interest since they cover a broad range of Pb isotopes, including ^{208}Pb. These excitation functions are for α-induced fission of ^{199}Hg, ^{200}Hg, ^{201}Hg, ^{202}Hg, ^{204}Hg and ^{204}Pb, forming the compound nuclei ^{203}Pb, ^{204}Pb, ^{205}Pb, ^{206}Pb, ^{208}Pb and ^{208}Po. Unfortunately, the analysis of ref. [13] cannot be applied directly to these systems due to the dramatic onset of shell effects near Z = 82 and N = 126.

We have, however, found an approach that, not only accommodates the shell effects altogether, allowing us to apply the method of ref. [13], but also extracts values for the shell effects which are independent of those obtained from the ground state masses. Furthermore, this approach allows one to visualize deviations in the level densities from the Fermi gas predictions at excitation energies only a few MeV over the fission saddle point, probably related to local shell and pairing effects.

In order to illustrate the method used here, let us write the transition state fission cross section as follows:

$$\sigma_f = \sigma_0 \frac{\Gamma_f}{\Gamma_T} \approx \sigma_0 \frac{1}{\Gamma_T} \frac{T_s \rho_s(E - B_f - E_r^s)}{2\pi\rho_n(E - E_r^{gs})}, \tag{1}$$

where ρ_s and ρ_n are the saddle and ground state level densities, respectively; E is the excitation energy of compound nucleus; B_f is the fission barrier; T_s is the energy dependent temperatures at the saddle; E_r^s, E_r^{gs} are the saddle and ground state rotational energies; σ_0 is the compound nucleus formation cross section.

Equation 1 can be rewritten as:

$$\frac{\sigma_f}{\sigma_0} \Gamma_T \frac{2\pi\rho_n(E - E_r^{gs})}{T_s} = \rho_s(E - B_f - E_r^s). \tag{2}$$

By evaluating the left hand side of this equation, using experimental data and standard physics, we obtain, in the right hand side, the level density at the saddle point. Using for simplicity the form

$$\rho(E) \propto \exp 2\sqrt{aE}, \tag{3}$$

we obtain:

$$\ln\left[\frac{\sigma_f}{\sigma_0} \Gamma_T \frac{2\pi\rho_n(E - E_r^{gs})}{T_s}\right] = 2\sqrt{a_f(E - B_f - E_r^s)}. \tag{4}$$

Thus, plotting the left-hand side versus $\sqrt{E - B_f - E_r^s}$ we should obtain a straight line representing the transition state null hypothesis. This is the equation that permitted the scaling of all the excitation functions in ref. [13].

In our mass region and excitation energy range, the neutron width dominates the total decay width:

$$\Gamma_T = \Gamma_n + \Gamma_p + \Gamma_\alpha + \cdots \approx \Gamma_n \approx KT_n^2 \frac{\rho_n(E - B_n - E_r^{gs})}{2\pi\rho_n(E - E_r^{gs})}, \tag{5}$$

where B_n is the last neutron binding energy; T_n is the temperature after neutron emission; $K = \frac{2m_n R^2 g'}{\hbar^2}$ with spin degeneracy $g' = 2$.

For the fission excitation functions considered here, however, the strong shell effects make the approximation $\rho_n(E - B_n - E_r^{gs}) \propto \exp 2\sqrt{a_n(E - B_n - E_r^{gs})}$ a very poor one. Attempts[14] to fit these excitation functions with such a functional form were successful only very near the barrier, and at the cost of extravagantly high values of a_f/a_n (up to 1.5). The situation improved substantially when the level density ρ_n was numerically calculated using the Nilsson shell model and the BCS Hamiltonian. In this case, the excitation functions could be fitted in their entirety and good barriers extracted[16, 17].

In these fission excitation functions, the lowest excitation energy for the residual nucleus after neutron emission is typically 15-20 MeV, possibly high enough for the level density to assume its asymptotic form[18]:

$$\rho_n(E - B_n - E_r^{gs}) \propto \exp 2\sqrt{a_n(E - B_n - E_r^{gs} - \Delta_{shell})}, \tag{6}$$

where Δ_{shell} is the ground state shell effect of the daughter nucleus after neutron emission. For the level density at the saddle point ρ_s, the problems should be far less serious. On the one hand, the large saddle deformations imply small shell effects. On the other, by its nature the saddle locates itself in between maxima and minima in the potential energy surface. Although deviations due to pairing may be expected at very low excitation energies, it should be safe to use:

$$\rho_s(E - B_f - E_r^s) \propto \exp 2\sqrt{a_f(E - B_f^* - E_r^s)}. \tag{7}$$

In the equation above, $B_f^* = B_f + \frac{1}{2}g\Delta_0^2$ for even-even nuclei and $B_f^* = B_f + \frac{1}{2}g\Delta_0^2 - \Delta_0$ for odd A nuclei, where Δ_0 is the saddle gap parameter and g the density of doubly degenerate

single particle levels at the saddle. In other words, B_f^* represents the unpaired saddle energy. Therefore for the scaling of the fission probabilities we can still attempt to use eq. 4, provided that eqs. 6 & 7 are employed for the level densities for the nucleus after neutron emission and at the saddle point, respectively. In order to implement the scaling we need the quantities B_f^* and Δ_{shell}.

A three parameter fit of the fission excitation functions with eq. 1 can be readily done, assigning, for instance, the value $a_n = A/8$ and using as fitting variables a_f/a_n, B_f^* and Δ_{shell}. In order to insure the applicability of eqs. 6 & 7 the lowest points of the experimental excitation functions were left out. In our fitting, σ_0 and the corresponding maximum angular momentum ℓ_{max} were calculated with an optical model[14], and E_r^s was computed assuming a configuration of two nearly touching spheres separated by 2 fm. This fitting was successfully performed for fourteen isotopes in the lead region (see Fig. 1). The best fit parameters are given in Table 1.

We begin by discussing the values of Δ_{shell} obtained in this manner for the daughter nuclei produced by neutron evaporation. In Fig. 2, we plot these values of Δ_{shell} versus the corresponding values obtained as the difference of the ground state mass and the corresponding liquid drop value. The observed correlation is excellent. Its importance can be better appreciated if one remembers how difficult it is to establish a good liquid drop baseline. The Δ_{shell} values obtained from the ground state masses[19-21] represent the culmination of over 30 years of effort. Over the years these Δ_{shell} values have changed quite substantially because of the reasons given above. The present shell corrections are obtained in a totally independent way, which, in contrast to the standard procedure[19] is completely local, namely it depends only on the properties of the nucleus under consideration.

In order to attempt the scaling suggested by eq. 4, we rewrite eq. 4 as:

$$\frac{1}{2\sqrt{a_n}}\ln\left[\frac{\sigma_f}{\sigma_0}\Gamma_T \frac{2\pi\rho_n(E-E_r^{gs})}{T_s}\right] = \frac{\ln R_f}{2\sqrt{a_n}} = \sqrt{\frac{a_f}{a_n}(E-B_f^*-E_r^s)}. \qquad (8)$$

Now we use this equation by introducing the experimental fission cross section σ_f, the effective barrier B_f^*, the shell effect Δ_{shell}, and $a_n = A/8$. One should note that we do not use the values of a_f/a_n obtained from the fit. Plotting the left-hand side of the above equation versus $\sqrt{E - B_f^* - E_r^s}$ leads to the remarkable results shown in Fig. 3. All of the excitation functions for fourteen different compound nuclei reduce beautifully to a single line. This scaling extends well over seven orders of magnitude in the fission probability and is even better than that observed in ref. [13] for complex fragment emission, despite the fact that the systems cover a region in A and Z where shell effects vary dramatically. The straight line, which is a linear fit to all but the two or three lowest data points, passes through zero quite accurately, and its slope is near 45° indicating that the ratio a_f/a_n is very close to unity. The universality of the scaling and the lack of deviation from a straight line over the entire energy range, except for the very lowest energies, indicates that the transition state null hypothesis and eqs. 6 & 7 hold extremely well.

While it must be stressed that the observed scaling is an empirical fact, the equation that suggested it (eq. 4), implies a dominance of first chance fission. Calculations verify that first chance fission dominates completely at the lower energies. Near the upper energy range, first chance fission still accounts for a large part of the cross sections with some uncertainties associated with the uncertainties in the nuclear parameters (barriers, shell effects, etc.) for the higher chance fissioning nuclei.

It is instructive now to investigate the effect of a delay time on the the first chance fission probability. In Fig. 4 calculations for a range of transient times are compared with the ^{201}Tl data that cover compound nucleus life-times from 10^{-16} to 10^{-20} seconds. Assuming a step function for the transient time effects, the fission width can be written as:

$$\Gamma_f = \Gamma_f^{(\infty)} \int_0^\infty \lambda(t) e^{-t/\tau_{CN}} dt = \Gamma_f^{(\infty)} e^{-\tau_D/\tau_{CN}} , \qquad (9)$$

where $\lambda(t) = 0$ $(t < \tau_D)$ and $\lambda(t) = 1$ $(t \geq \tau_D)$; τ_D is the transient time; $\Gamma_f^{(\infty)}$ denotes the transition state fission width; and τ_{CN} is the compound nucleus life time. In Fig. 4 no indication of transient times longer than 3×10^{-20} seconds is apparent.

The extracted barriers B_f^* can be compared to the true barriers B_f shown in Table 1. In general, the differences are 2 - 4 MeV larger and likely to be related to the pairing energy at the saddle, and are more or less consistent with the relationship $B_f^* = B_f + \frac{1}{2}g\Delta_0^2$ for even-even nuclei and $B_f^* = B_f + \frac{1}{2}g\Delta_0^2 - \Delta_0$ for odd A nuclei for a value of $\Delta_0 \sim 0.7$ MeV. For the three Os isotopes, B_f^* is similar to B_f, due to the fact that these excitation functions do not extend sufficiently close to the true barriers. The deviations of the data from the straight line, visible at low energies in Fig. 3, are most likely due to deviations of the saddle point level densities from the Fermi gas values due to pairing effects.

In summary, we have shown that the fission excitation functions for fourteen compound nuclei covering a mass range A = 186 - 213 can be scaled exactly according to the transition state prediction onto a single straight line, once the shell effects are accounted for. The extracted shell effects correlate closely with those obtained from the ground state masses. No evidence for the effects of transient times longer than 3×10^{-20} seconds is found.

Acknowledgment

Present address:

[a]Earth Sciences Division, Lawrence Berkeley Laboratory, Berkeley, CA 94720

Table 1

Nuclide	B_f[1]	B_f^*	a_f/a_n	Δ_{shell}[2]	Δ_{FRDM}[2,3]
^{213}At	17.0	20.1	1.036	9.7 ± 1.5	8.7
^{212}Po	19.5	22.6	1.028	10.9 ± 1.5	10.0
^{211}Po	19.7	23.1	1.028	13.4 ± 1.5	10.8
^{210}Po	20.5	25.2	1.029	12.7 ± 1.5	10.7
^{208}Po		23.5	1.055	10.0 ± 1.5	9.0
^{208}Pb		27.1	1.000	10.2 ± 2.0	12.7
^{206}Pb		26.4	1.022	9.8 ± 2.0	11.0
^{205}Pb		26.4	1.001	11.8 ± 2.0	10.0
^{204}Pb		25.7	1.022	9.8 ± 2.0	9.1
^{203}Pb		24.1	1.021	10.0 ± 2.0	8.2
^{201}Tl	22.3	24.2	1.025	8.7 ± 1.5	7.5
^{188}Os	24.2	23.2	1.025	1.4 ± 2.0	2.2
^{187}Os	22.7	22.7	1.022	3.2 ± 2.0	1.9
^{186}Os	23.4	22.4	1.020	1.5 ± 2.0	1.8

[1]Taken from refs. [16, 17]

[2]Shell correction for the daughter nucleus after evaporation of a neutron.
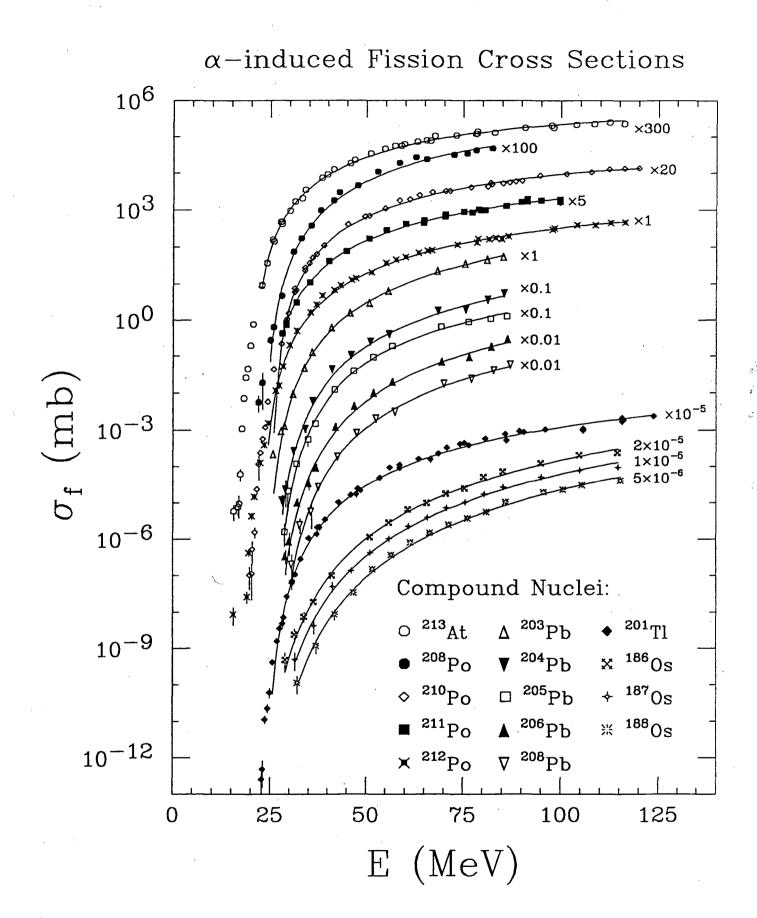
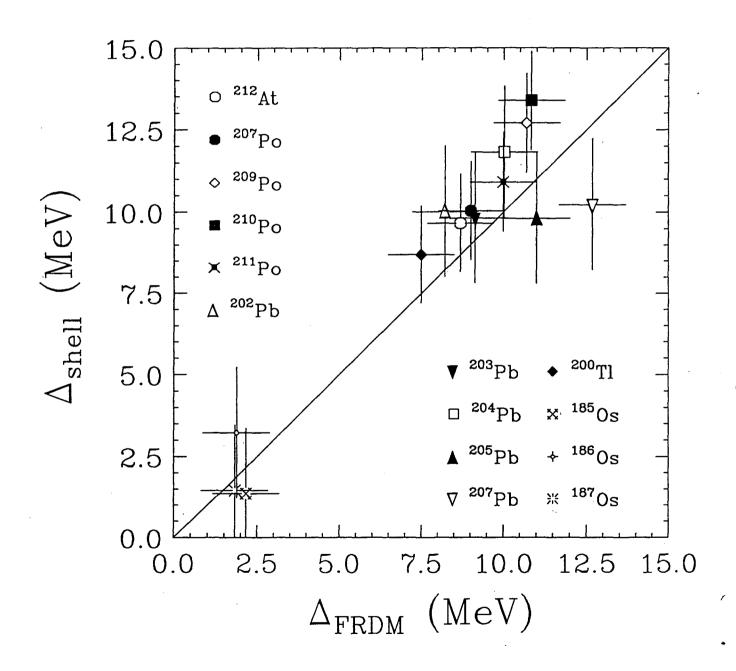[3]Taken from ref. [19]. The possible systematic error is of the order of ± 1 MeV.
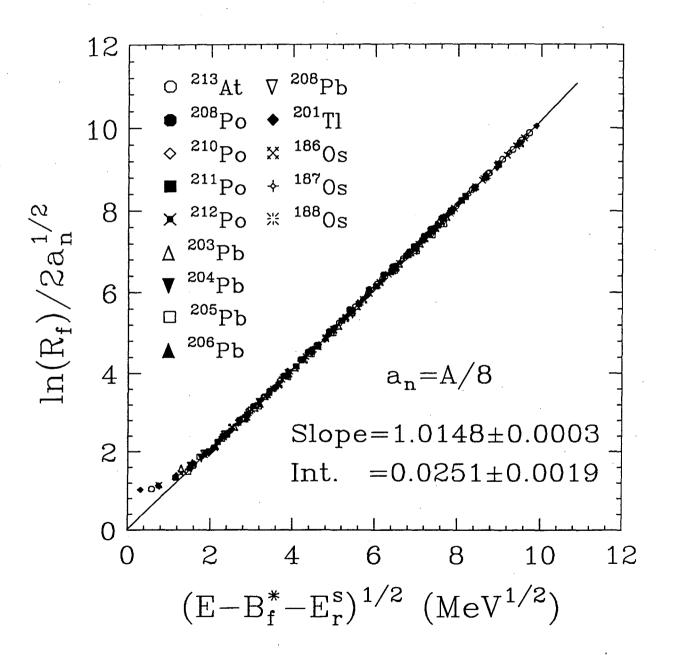
Figure Captions:

Fig.1. Fission excitation functions of the compound nuclei ^{186,187,188}Os, ^{201}Tl, ^{203,204,205,206,208}Pb, ^{208,210,211,212}Po, and ^{213}At formed in α-induced reactions. The solid lines correspond to the fits as described in the text. Error bars are shown when they exceed the size of the symbols.

Fig.2. Shell corrections Δ_{shell}, for the daughter nuclei (A_{CN} - n), extracted from fits to the excitation functions shown in Fig. 1 plotted against the values determined from the ground state masses[19]. The diagonal line is to guide the eye.

Fig. 3. a) The quantity $\ln R_f$ divided by $2\sqrt{a_n}$ vs the square root of the intrinsic excitation energy over the saddle for fission of the compound nuclei: ^{186,187,188}Os, ^{201}Tl, ^{203,204,205,206,208}Pb, ^{208,210,211,212}Po, and ^{213}At. The straight line is a linear fit to all but the lowest two or three data points.

Fig. 4. Same as Fig. 3 for the compound nucleus ^{201}Tl. The compound nucleus life time τ_{CN} is indicated on the top. The straight line is a linear fit to all but the lowest three data points. The three additional solid lines represent calculations (see text) assuming that no fission occurs during the transient times of 3×10^{-20}, 10^{-19}, and 5×10^{-19} seconds, respectively.
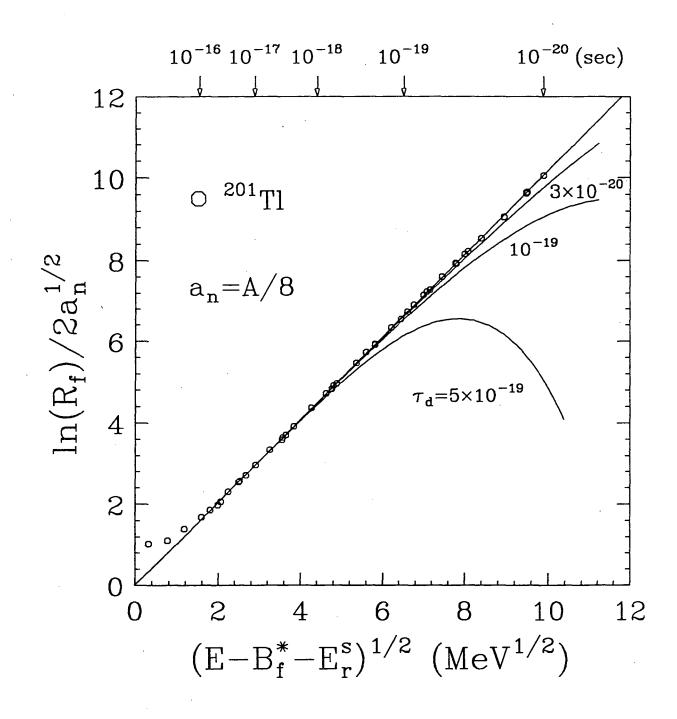
References:

[1] N. Bohr and J. A. Wheeler, Phys. Rev. **56**, 426 (1939).

[2] D. Hilscher and H. Rossner, Ann. Phys. Fr. **17**, 471-552 (1992), and references therein.

[3] P. Paul and M. Thoennessen, Ann. Rev. Nucl. Part. Sc. **44**, 65 (1994), and references therein.

[4] M. Thoennessen and G. F. Bertsch, Phys. Rev. Lett. **71**, 4303 (1993).

[5] P. Grange and H. A. Weidenmüller, Phys. Lett. **B96,** 26 (1980).

[6] P. Grange, J.-Q. Li, and H. A. Weidenmüller, Phys. Rev. **C27**, 2063 (1983).

[7] H. A. Weidenmüller and J.-S. Zhang, Phys. Rev. **C29**, 879 (1984).

[8] P. Grange, et al, Phys. Rev. **C34**, 209 (1986).

[9] Z.-D. Lu, et al, Z. Phys. A **323**, 477 (1986).

[10] Z.-D. Lu, et al, Phys. Rev. **C42**, 707 (1990).

[11] D. Cha and G. F. Bertsch, Phys. Rev. **C46**, 306 (1992).

[12] P. Frobrich, I. I. Gontchar, and N. D. Mavlitov, Nucl. Phys. **A556**, 281 (1993).

[13] L. G. Moretto, K. X. Jing, and G. J. Wozniak, Phys. Rev. Lett **74**, 3557 (1995).

[14] A. Khodai-Joopari, Ph.D., University of California, Berkeley (1966).

[15] D. S. Burnett, et al, Phys. Rev. **134**, B952 (1964).

[16] L. G. Moretto, S. G. Thompson, J. Routti, and R. C. Gatti, Phys. Lett. **B38**, 471 (1972).

[17] L. G. Moretto, in *Physics and Chemistry of Fission 1973*, vol. I, ed. (International Atomic Energy Agency, Vienna, 1974) p. 329.

[18] J. R. Huizenga and L. G. Moretto, Ann. Rev. Nucl. Sci. **22**, 427 (1972).

[19] P. Möller, J. R. Nix, W. D. Myers, and W. J. Swiatecki, Los Alamos National Laboratory LA-UR-3083 (1994).

[20] W. D. Myers and W. J. Swiatecki, Lawrence Berkeley Laboratory LBL-36557 (1994).

[21] W. D. Myers and W. J. Swiatecki, Lawrence Berkeley Laboratory LBL-36803 (1994).

α-induced Fission Cross Sections

Compound Nuclei:

○ ^{213}At	△ ^{203}Pb	◆ ^{201}Tl
● ^{208}Po	▼ ^{204}Pb	✳ ^{186}Os
◇ ^{210}Po	□ ^{205}Pb	✛ ^{187}Os
■ ^{211}Po	▲ ^{206}Pb	✳ ^{188}Os
✶ ^{212}Po	▽ ^{208}Pb	

Figure 1
11

Figure 2
12

Figure 3
13

Figure 4
14